Available online at www.sciencedirect.com
SCIENCE DIRECT
Mathematical and Computer Modelling 43 (2006) 582–591
MATHEMATICAL AND COMPUTER MODELLING
www.elsevier.com/locate/mcm

Spectral element modeling of semiconductor heterostructures

G. von Winckel[a,*], S. Krishna[a], E.A. Coutsias[b]

[a] *Center for High Technology Materials, University of New Mexico, Albuquerque, NM 87131, United States*
[b] *Department of Mathematics and Statistics, University of New Mexico, Albuquerque, NM 87131, United States*

Received 2 May 2005; accepted 5 May 2005

Abstract

We present a fast and efficient spectral method for computing the eigenvalues and eigenfunctions for a one-dimensional piecewise smooth potential, as arises in the case of epitaxially grown semiconductor heterostructures. Many physical devices such as quantum well infrared photodetectors and quantum cascade lasers rely upon transitions between bound and quasi-bound or continuum states; consequently it is imperative to determine the resonant spectrum as well as the bound states. Instead of trying to approximate radiation boundary conditions, our method uses a singular mapping combined with deforming the coordinate system to a contour in the complex plane to construct semi-infinite elements of perfectly matched layers. We show that the PML elements need not be based on a smooth contour to absorb outward-propagating waves and that the resonant eigenvalues can be computed to machine precision. A fast means of computing inner products and expectations of quantum mechanical operators with quadrature accuracy in the spectral domain is also introduced.

Keywords: 1D Schrödinger equation; Eigenvalue problems; Spectral methods; Complex coordinate scaling; Semiconductor modeling

1. Introduction

With modern advances in epitaxial growth technology, it has become possible to fabricate a wide range of semiconductor devices such as quantum well infrared photodetectors, semiconductor lasers, and resonant tunneling diodes. These devices are all examples of heterostructures. Semiconductor heterostructures consist of many planar layers of materials with differing electrical properties. The layer widths in such devices are on the order of nanometers and consequently the behavior of electrons in these structures is described by quantum mechanics.

Two typical uses of heterostructures in optoelectronic devices, e.g. in photodetectors or photoemitters, involve transitions of electrons between bound and continuum states. In photodetectors, photons promote electrons from bound states to the continuum, whereas in photoemitters, photons are produced by electrons relaxing from the continuum (see Fig. 1) into bound states [1]. The interaction between electrons and photons in such devices, is modeled using time-dependent perturbation theory with Fermi's Golden Rule [2]. This approach reduces the quantum electrodynamics description of the process to the study of the Schrödinger equation for a single electron in a potential

* Corresponding author.
E-mail addresses: gregvw@chtm.unm.edu (G. von Winckel), skrishna@chtm.unm.edu (S. Krishna), vageli@math.unm.edu (E.A. Coutsias).

0895-7177/$ - see front matter © 2005 Elsevier Ltd. All rights reserved.
doi:10.1016/j.mcm.2005.05.028

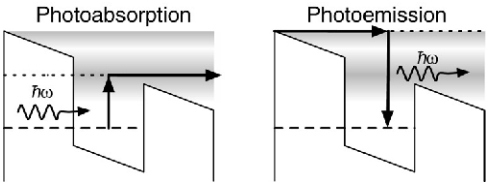

Fig. 1. *Left:* Electrons in bound states can be excited to the continuum by an incident photon. *Right:* Electrons in the continuum can relax to bound states by emitting a photon.

well. Since the layers are thin compared to the lateral dimensions of the structure, the problem may be treated using the one-dimensional Schrödinger equation in the direction normal to the planes, with a piecewise smooth potential. In this approximation, the important quantities to compute are the eigenvalues and eigenfunctions for the time-independent problem. One must typically compute many eigenfunctions and inner products to model change in electron energy states due to photoabsorption or emission. For these cases, the continuum states are not square-integrable and must be weighted by the spectral density function. Frequently in the literature, the spectral density function used is for the free particle approximation, when it actually depends on the complex spectrum of the Schrödinger operator [3]. As a rule, the bound eigenfunctions and their energies are the easiest to compute. Computation of the spectral density can be challenging, both as regards size and convergence. The four basic approaches are: constructing approximate radiation conditions [4,5], shooting methods [6,7], introducing a complex "optical" potential [8], and complex coordinate scaling [9–12]. One of the techniques that has been used to arrive at relevant properties of the spectral density involves computation of eigenstates of the Schrödinger operator with complex energies, the so-called *resonance spectrum* [13]. The corresponding *resonant eigenfunctions* exhibit exponential growth at infinity. Thus, determining the optoelectronic properties of heterostructures requires the solution of two kinds of discrete eigenproblems: the standard, bound state problem with square-integrable eigenfunctions and the resonant problem with unbounded eigenfunctions. The spectral element method presented here provides a fast-converging sparse matrix approximation to the Schrödinger eigenproblem. It affords a simple way to compute inner products in quadrature and with the addition of semi-infinite absorbing layers, it is a trivial matter to resolve the resonant spectrum as well.

Spectral methods have been most popular in the field of computational fluid dynamics [14], although they are especially well suited to quantum mechanical eigenvalue problems. Even so, the literature for spectral methods in quantum mechanics is relatively limited. More commonly, finite difference [4] schemes or shooting methods such as the transfer matrix approach [6,7] have been employed in computing eigenvalues and eigenfunctions for quantum mechanical potentials. Spectral methods have been employed to compute eigenfunctions for atomic [15] and oscillator [16] potentials with great success. Here we introduce a spectral element approach based on Lanczos's tau method [17] with the Legendre basis for solving the one-dimensional time-independent Schrödinger equation (TISE) with arbitrary piecewise smooth potentials in unbounded domains. This approach allows for a numerically robust and fast computation of the eigenvalues and eigenvectors of the Hamiltonian operator for potentials with an arbitrary number of discontinuities typified by epitaxially grown quantum semiconductor devices. The spectral method offers a substantial advantage over shooting methods in that it is possible to simultaneously compute as many eigenfunctions and eigenvalues as desired. While this is also true for finite difference schemes, we shall see that for a given tolerable error, the spectral method requires matrices which are usually orders of magnitude smaller than the corresponding finite difference matrices. Since the energy band profile of an epitaxially grown structure is piecewise smooth, spectral element methods guarantee exponential convergence of the solution [19], whereas finite difference methods will converge only algebraically.

The method of discretization on elements of finite length is the Legendre tau method. This approach is preferred over collocation and Galerkin approximations for three reasons: the flexibility in imposing boundary conditions, ease of treating variable coefficients, and the availability of integration preconditioners [20,21] which gives rise to a quasi-banded eigenvalue problem. In semiconductor heterostructures, the potential profile is typically well approximated by a low order polynomial or rational function wherever it is continuous. For this situation, the eigenvalue problem will be sparser than for a collocation or Galerkin discretization. This becomes important for modeling structures with many different layers such as superlattices and vertical cavity surface emitting lasers, as the sparse eigenvalue problem can be more rapidly solved with the numerical library ARPACK [22].

Our multi-domain approach combined with singular mapping allows one to treat the asymptotic regions exactly as any other elements. By deforming the coordinates to a contour in the complex plane, we can find a trajectory along which the resonant eigenfunctions decay and have a convergent expansion which allows the efficient computation of the resonant spectrum.

In Section 2, the basic Legendre tau formulation is introduced for the one-dimensional Schrödinger equation with a smooth potential. Section 3 generalizes the approach to the case where the potential has discontinuities by decomposing the domain with spectral elements. Section 4 deals with the Schrödinger problem on the whole line as well as the resolution of resonant states through complex scaling. Finally, a method for computing scattering states and inner products is described.

2. Formulation

The TISE in one dimension is

$$\left\{-\frac{\hbar^2}{2}\frac{\mathrm{d}}{\mathrm{d}x}\frac{1}{m^*(x)}\frac{\mathrm{d}}{\mathrm{d}x}+V(x)\right\}\psi(x)=E\psi(x). \tag{1}$$

Scaling out the physical constants leads to the standard form and we get the Sturm–Liouville problem:

$$\left\{-\frac{\mathrm{d}}{\mathrm{d}x}p(x)\frac{\mathrm{d}}{\mathrm{d}x}+q(x)-\lambda\right\}\psi(x)=0,\quad p(x)=\frac{m_0}{m^*(x)},\quad q(x)=\frac{2m_0}{\hbar^2}V(x),\quad \lambda=\frac{2m_0}{\hbar^2}E. \tag{2}$$

The transformation $\tilde{x}=\frac{2x-a-b}{b-a}$ maps a domain $[a,b]$ onto the unit interval $[-1,1]$. The Schrödinger eigenproblem is then solved numerically using Lanczos's tau method [17] which is described in detail below. Let N be the order of truncation so that on the unit interval the Legendre–Gauss–Lobatto (LGL) nodes are

$$\{x_k \mid (1-x_k^2)P_N'(x_k)=0 \mid 0\le k\le N\}. \tag{3}$$

The known functions $p(\tilde{x})$ and $q(\tilde{x})$ are sampled at the LGL nodes and are expanded in terms of Legendre polynomials [19]:

$$q_N(\tilde{x})=\sum_{j=0}^{N}\hat{q}_j P_j(\tilde{x}). \tag{4}$$

The values that $q(\tilde{x})$ takes at the LGL nodes are stored in a column vector $\mathbf{q}_N$. The vectors of nodal values and expansion coefficients are related by the Legendre Vandermonde matrix $\mathbf{q}_N=\mathbf{V}\hat{\mathbf{q}}$, whose elements are $V_{ij}=P_j(x_i)$. The functions $p(x)$, $q(x)$ and $w(x)$ have convolution matrix representations [20] of the form

$$\mathbf{Q}=\sum_{j=0}^{N}\hat{q}_j\mathbf{P}_j, \tag{5}$$

where the $\mathbf{P}_j$ are computed from the Legendre recurrence relation [23] $(j+1)\mathbf{P}_{j+1}=(2j+1)\mathbf{X}\mathbf{P}_j-j\mathbf{P}_{j-1}$ where $\mathbf{P}_0=\mathbf{I}$ and $\mathbf{P}_1=\mathbf{X}$ are the identity and x-convolution matrices. The entries of $\mathbf{X}$ are obtained from the Legendre recurrence [20]. Writing the EVP as a matrix equation,

$$\left\{-\frac{4}{(b-a)^2}\mathbf{D}\,[\mathbf{P}\mathbf{D}]+\mathbf{Q}\right\}\hat{\mathbf{u}}=\lambda\hat{\mathbf{u}} \tag{6}$$

where the differentiation operator has discretized as the $\mathbf{D}$ matrix. It is often desirable to convert to integration-preconditioned form [21], which improves the convergence, but more importantly renders the generalized eigenproblem more sparse, which is of particular value when using a sparse eigenvalue solver such as ARPACK [22]. Two important identities are $\mathbf{D}\mathbf{X}-\mathbf{X}\mathbf{D}=\mathbf{I}$ and $\mathbf{B}_{[1]}\mathbf{D}=\mathbf{I}_{[1]}$ where $\mathbf{B}_{[1]}$ is the integration matrix and is the pseudoinverse of $\mathbf{D}$. We use the notation $\mathbf{A}_{[n]}$ for the matrix $\mathbf{A}$ with the first n rows set to zero. To convert to integrator

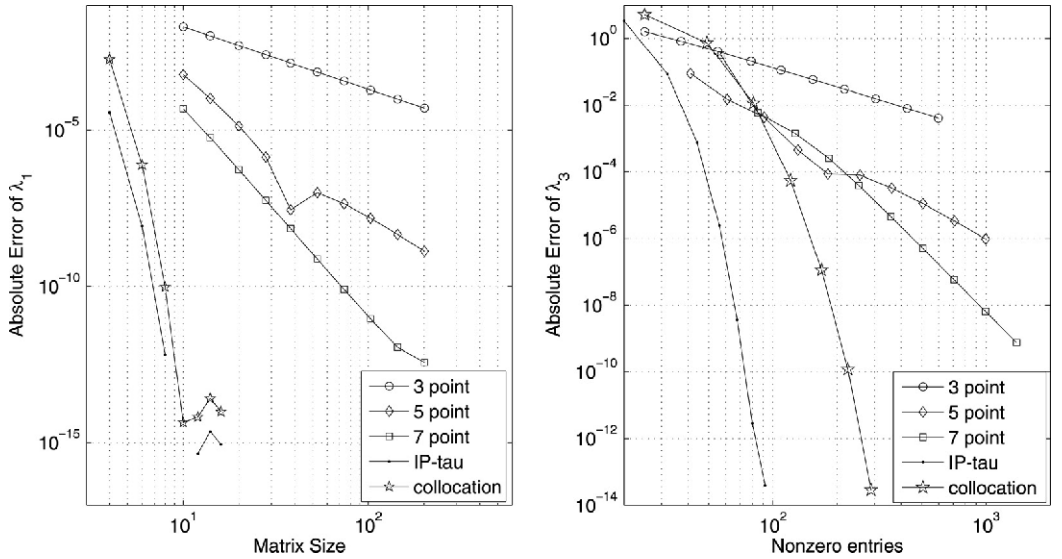

Fig. 2. *Left*: Convergence of the first eigenvalue of $-u'' = \lambda u$ with $u(\pm 1) = 0$ using three-, five-, and seven-point centered differences versus integration-preconditioned Legendre tau and Legendre collocation as a function of matrix size (grid points or polynomials). *Right:* Convergence of the third eigenvalue as a function of nonzero matrix elements.

form, the second derivative must be brought to the left of $\mathbf{P}$; to do this, the necessary identity is $\mathbf{PD} = \mathbf{DP} - \mathbf{P}'$. The prime notation indicates

$$\mathbf{P}' = \sum_{j=0}^{N} \hat{p}'_j \mathbf{P}_j, \quad \hat{\mathbf{p}}' = \mathbf{D}\hat{\mathbf{p}}. \tag{7}$$

The integration $\mathbf{B}_{[2]}$ matrix is then applied twice and letting

$$\mathbf{L}_{[2]} = -\frac{4}{(b-a)^2}[\mathbf{P}_{[2]} + \mathbf{B}_{[2]}\mathbf{P}'] + \mathbf{B}_{[2]}^2\mathbf{Q} \tag{8}$$

we obtain the generalized eigenvalue problem (GEVP), $\mathbf{L}_{[2]}\hat{\mathbf{u}} = \lambda \mathbf{B}_{[2]}^2\hat{\mathbf{u}}$. Now we must impose the two tau conditions since the DE is second order. This is accomplished by inserting Dirichlet operators for the endpoints into the first two rows of $\mathbf{L}$. These operators are described in the next section. The GEVP is solved numerically using the QZ algorithm [18].

To demonstrate the convergence, we show the absolute error versus polynomial truncation for an infinite potential well on the unit interval. The convergence of the tau, collocation, and finite difference (FD) schemes for the ground state makes the advantage of spectral methods immediately apparent. Fig. 2 demonstrates the convergence of the integration-preconditioned tau (IP-tau) method and collocation method with three-, five-, and seven-point FD schemes. One advantage of FD schemes is that although the matrix may be very large, it generally has banded or quasi-banded form, and consequently the matrix tends to be sparse. The sparsity of the FD matrices will generally not depend on the variable coefficients p and q of the discretized BVP. This is not the case with the IP-tau method, as the bandwidth of the matrices will increase as the variable coefficients increase in polynomial order. For heterostructure problems, this effect is typically small. With the availability of sparse solvers [22], a fairer comparison of the spectral and FD schemes is convergence as a function of matrix sparsity. This is demonstrated in the right plot in Fig. 2.

3. Multiple elements

While the spectral method produces optimal results approximating smooth functions, in most practical heterostructures, the potential is only smooth within a given epitaxial layer with potential discontinuities in the band edge corresponding to material interfaces. Legendre polynomials will converge to a discontinuous function

in the L_2 sense but not in L_∞ due to the Gibbs phenomenon [19]. Although there exist methods for filtering out Gibbs phenomena [24] and restoring spectral convergence, heterostructure problems are most efficiently solved using spectral elements since the discontinuities have known fixed locations. When there are multiple elements, there is a different discretized Hamiltonian operator for each element. A global solution is obtained by requiring that each local solution and its derivative equal the next local solution at the interface between elements.
Consider a discontinuous potential well

$$q(x) = \begin{cases} q_1 & : \quad -1 \le x < 0 \\ q_2 & : \quad 0 \le x \le 1 \\ \infty & : \quad |x| > 1 \end{cases} \tag{9}$$

letting for example $q_1 = 0$ and $q_2 = 100$. This gives two DEs where the solutions are coupled through boundary conditions at $x = 0$:

$$\begin{aligned} &\left\{-\frac{\mathrm{d}^2}{\mathrm{d}x^2} + q_{1,2}\right\} u_{1,2}(x) = \lambda u_{1,2}(x) \\ &u_1(-1) = 0, \quad u_2(+1) = 0 \\ &u_1(0) = u_2(0), \quad u_1'(0) = u_2'(0). \end{aligned} \tag{10}$$

Writing (10) as a matrix eigenproblem gives

$$\begin{aligned} &\mathbf{L}_{1,2}\hat{\mathbf{u}}_{1,2} = \lambda \mathbf{B}^2 \hat{\mathbf{u}}_{1,2} \\ &\boldsymbol{\delta}_-\hat{\mathbf{u}}_1 = 0, \quad \boldsymbol{\delta}_+\hat{\mathbf{u}}_2 = 0 \\ &\boldsymbol{\delta}_+\hat{\mathbf{u}}_1 - \boldsymbol{\delta}_-\hat{\mathbf{u}}_2 = 0 \\ &\alpha \boldsymbol{\nu}_+\hat{\mathbf{u}}_1 - \alpha \boldsymbol{\nu}_-\hat{\mathbf{u}}_2 = 0. \end{aligned} \tag{11}$$

The Dirichlet and Neumann operators are row vectors defined as

$$\begin{aligned} \boldsymbol{\delta}_+ &= \begin{bmatrix} P_0(x_0) & P_1(x_0) & P_2(x_0) & \cdots & P_N(x_0) \end{bmatrix} &&= \begin{bmatrix} 1 & 1 & 1 & 1 & 1 & 1 & \cdots \end{bmatrix} \\ \boldsymbol{\delta}_- &= \begin{bmatrix} P_0(x_N) & P_1(x_N) & P_2(x_N) & \cdots & P_N(x_N) \end{bmatrix} &&= \begin{bmatrix} 1 & -1 & 1 & -1 & 1 & 1 & \cdots \end{bmatrix} \\ \boldsymbol{\nu}_+ &= \begin{bmatrix} P_0'(x_0) & P_1'(x_0) & P_2'(x_0) & \cdots & P_N'(x_0) \end{bmatrix} &&= \begin{bmatrix} 0 & 1 & 3 & 6 & 10 & 15 & \cdots \end{bmatrix} \\ \boldsymbol{\nu}_- &= \begin{bmatrix} P_0'(x_N) & P_1'(x_N) & P_2'(x_N) & \cdots & P_N'(x_N) \end{bmatrix} &&= \begin{bmatrix} 0 & 1 & -3 & 6 & -10 & 15 & \cdots \end{bmatrix}. \end{aligned} \tag{12}$$

Typically the elements will not be of the same length and the effective masses in the two regions may be different, so the Neumann operators must be scaled accordingly. Now the equations in (10) can be written as a GEP:

$$\left(\begin{array}{c|c} \boldsymbol{\delta}_- & 0 \\ \boldsymbol{\delta}_+ & -\boldsymbol{\delta}_- \\ \mathbf{L}_1 & 0 \\ \hline 0 & \boldsymbol{\delta}_+ \\ -\boldsymbol{\nu}_+ & \boldsymbol{\nu}_- \\ 0 & \mathbf{L}_2 \end{array}\right) \left(\begin{array}{c} \hat{\mathbf{u}}_1 \\ \\ \hline \\ \hat{\mathbf{u}}_2 \end{array}\right) = \lambda \left(\begin{array}{c|c} \mathbf{B}_{[2]}^2 & 0 \\ \hline 0 & \mathbf{B}_{[2]}^2 \end{array}\right) \left(\begin{array}{c} \hat{\mathbf{u}}_1 \\ \hline \hat{\mathbf{u}}_2 \end{array}\right). \tag{13}$$

This approach generalizes to any number of elements where matching conditions on the solution and its derivative are imposed at the interfaces. In general, the left matrix of the pencil (13) will be block tridiagonal and the right matrix will be block diagonal. It should also be mentioned that although we have chosen the same polynomial truncation for each element, this is by no means necessary. Typically, one may wish to use a larger truncation with longer elements or in elements where the wavefunction is expected to oscillate rapidly over space.

4. Unbounded domains

There are several approaches to handling the unbound domain problem. For exponentially decaying functions, simple domain truncation will typically work. Unfortunately, if the domain is truncated too close to the region of

interest, it will affect the local solution, whereas if it is truncated too far away, it will require more polynomials to resolve the overall behavior. For the eigenvalue problem, each bound eigenfunction decays at a different rate, so there is no best distance at which to truncate the domain. Some authors have avoided this problem by imposing a radiation condition at the exterior boundary instead of a simple Dirichlet condition. By using the dispersion relation for the Schrödinger equation, one can write a Robin condition which depends on the eigenvalue. Unfortunately, since the equation is parabolic, there will be a square-root dependence on energy in the exact boundary operator. Shibata [4] uses a linear least-squares fit to the group velocity in the boundary condition. That approach is improved somewhat by using a bi-linear Padé approximant [5] instead; however, the eigenproblem is weakly ill-posed with respect to such radiation conditions. Due to the square-root singularity, no low order polynomial or rational approximation will give a good fit over a wide range of energies. Even a bi-cubic Padé approximant can produce eigenvalues with an error as large as 10% and this is at the expense of tripling the size of the system. Instead, we propose using semi-infinite PML elements to absorb all outward-propagating waves. This approach is detailed in the next two sections.

4.1. Rational mapping for bound states

Now we consider an approach [25] which maps the semi-infinite intervals $(-\infty, -R]$ and $[+R, \infty)$ to the unit interval (see Fig. 3). This is accomplished using a rational map. Let $y_- : [-\infty, -R] \mapsto [-1, 1]$ and $y_+ : [+R, +\infty] \mapsto [-1, 1]$. These maps and their inverses are

$$y_\pm = \pm 2\left(\frac{x \mp R}{x \pm R}\right) \mp 1, \quad x = R\frac{y_\pm \pm 3}{1 \mp y_\pm}. \tag{14}$$

The mapped derivatives are

$$\frac{\partial}{\partial x} = \frac{1}{4R}(y_\pm \mp 1)^2 \frac{\partial}{\partial y_\pm}, \quad \frac{\mathrm{d}^2}{\mathrm{d}x^2} = \frac{1}{8R^2}(y_\pm \mp 1)^3 \frac{\mathrm{d}}{\mathrm{d}y_\pm} + \frac{1}{16R^2}(y_\pm \mp 1)^4 \frac{\mathrm{d}^2}{\mathrm{d}y_\pm^2}. \tag{15}$$

One can then construct a three-element scheme similar to (13) where there will be one sub-matrix each for the right and left asymptotic regions and a sub-matrix for the quantum well element. The matchings of the Dirichlet conditions and Neumann conditions are exactly as before because the mappings are precisely linear at the points $x = \pm R$. We then implement this approach and examine the convergence of the first and third eigenvalues of a finite potential well with depth $q_0 = 100$ and width $L = 2$. The integrator-preconditioned operators for the left $(-)$ and right $(+)$ asymptotic regions are

$$\mathbf{L}_\pm = -\frac{1}{16R^2}(\mathbf{X} \mp \mathbf{I})^4 + \frac{3}{8R^2}\mathbf{B}(\mathbf{X} \mp \mathbf{I})^3 + \mathbf{B}^2\left[q_0\mathbf{I} - \frac{3}{8R^2}(\mathbf{X} \mp \mathbf{I})^2\right] \tag{16}$$

whereas the operator for the quantum well is simply $-\mathbf{I}$. The left-hand side of the resulting matrix pencil is

$$l.h.s. = \left(\begin{array}{c|c|c} \boldsymbol{\delta}_- & & \\ \boldsymbol{\delta}_+ & -\boldsymbol{\delta}_- & \\ \mathbf{L}_- & & \\ \hline \boldsymbol{\nu}_+ & -\boldsymbol{\nu}_- & \\ & -\boldsymbol{\nu}_+ & \boldsymbol{\nu}_- \\ & -\mathbf{I} & \\ \hline & -\boldsymbol{\delta}_+ & \boldsymbol{\delta}_- \\ & & \boldsymbol{\delta}_+ \\ & & \mathbf{L}_+ \end{array}\right) \tag{17}$$

and the right-hand side is simply block diagonal with three $\mathbf{B}_{[2]}^2$ blocks. The exact eigenvalues have been computed using the Newton–Raphson method. Additionally, we have computed $\lambda_{1,3}$ using domain truncation where an element of length $L = 15$ has been placed on either side of the quantum well. Fig. 4 demonstrates that both methods converge; however, the rational map gives spectral convergence whereas the truncated domain approach provides algebraic convergence. Both methods are limited to the calculation of bound states, as the Dirichlet conditions imposed by domain truncation will discretize the continuous spectrum into real bound states and destroy the resonances [13].

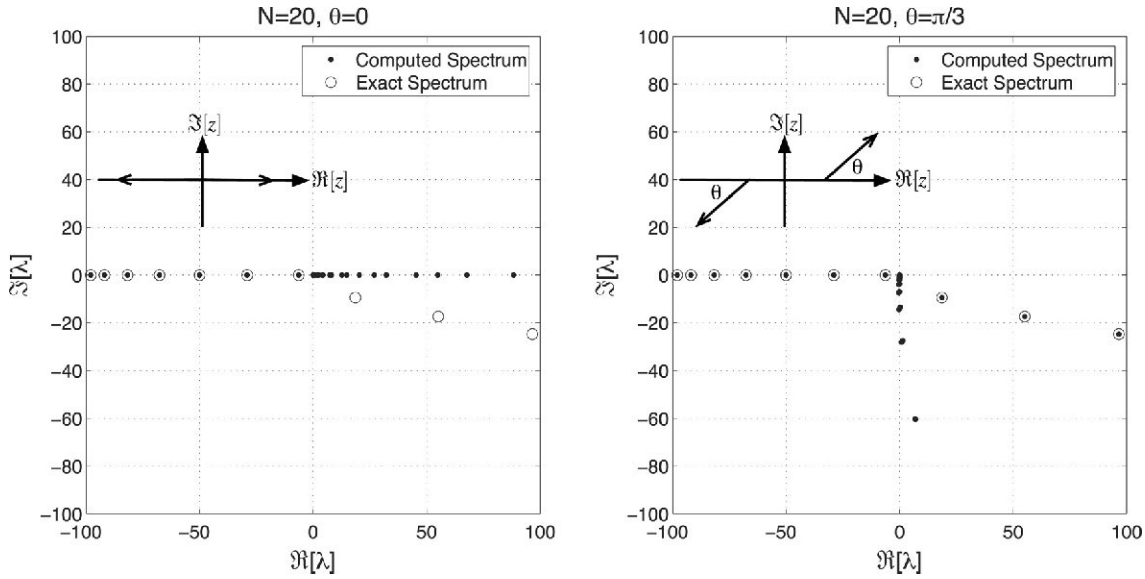

Fig. 3. Complex spectrum for the square finite potential quantum well. The domain is split into two semi-infinite elements and a finite element with 20 Legendre polynomials per element. On the left, no coordinate rotation is applied and only the bound states are resolved. On the right, the coordinates are rotated in the exterior elements by $\frac{\pi}{3}$ to obtain semi-infinite PML regions and the complex eigenvalues are resolved. *Note:* The pseudo-spectrum can be identified by its movement with respect to the scaling parameter θ.

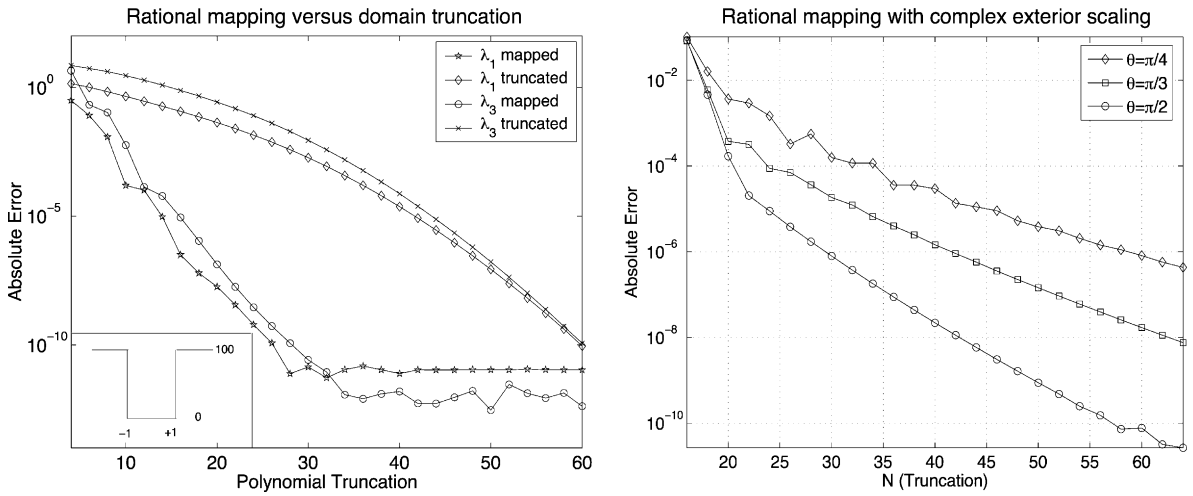

Fig. 4. *Left:* Absolute error of the first and third eigenvalues with rational mapping compared to domain truncation. For domain truncation, $L = 15$. *Right:* Absolute error of the first resonance for different coordinate rotations.

The rational mapping does not immediately work for unbound states since it will map a function which oscillates periodically on an infinite interval to a finite interval, thereby creating a function which has an essential singularity at a point in the domain. For unbound states we extend the mapping approach.

4.2. Computing resonances with complex coordinate deformations

For open quantum systems, it is possible for the Hamiltonian to have discrete complex eigenvalues embedded in the continuous spectrum. These resonances give rise to maxima in the spectral density. Typically, the resonant eigenvalues are denoted as $E_n = e_n - i\,\Gamma_n$, where $\Gamma_n = \hbar/\tau_n$ and τ_n is said to be the expected lifetime of the resonant state. These resonant states determine the spectral density function, or density of states, which appears as the weight for transitions

between states. For the purely bound case, the spectral density function is

$$\rho(E) = \sum_n \delta(E - E_n) \tag{18}$$

where $\delta(E - E_n)$ is the Dirac distribution. When resonant states are present, the delta distribution is generalized through the well-known relation

$$\lim_{\epsilon \to 0} \frac{1}{E - E_n + i\epsilon} = \mathcal{P}\left(\frac{1}{E - E_n}\right) - i\pi\delta(E - E_n). \tag{19}$$

Consequently, for the resonant states, $\Gamma \neq 0$ and the delta functions will be broadened into Lorentzian functions.

$$\delta(E - E_n) \to \frac{1}{\pi} \frac{\Gamma_n}{(E - e_n)^2 + \Gamma_n^2}. \tag{20}$$

If the coordinate x is taken along the real axis, the eigenfunctions diverge at large distances with oscillatory exponential growth. Since the coordinates are not a quantum mechanical observable, the spectrum is not affected by solving the eigenvalue problem along a different contour in the complex plane. This approach was first employed in quantum chemistry using coordinate rotation; see [26] and references therein. The standard example is the radial equation for the Coulomb potential where the r is replaced by $re^{i\theta}$. Complex coordinate rotation works well if the potential has a simple analytic continuation in the complex plane. For potentials which are locally complicated but asymptotically simple, Simon [9] introduced the method of complex exterior scaling, which has the form

$$r(x) = \begin{cases} x & \text{if } x \leq R_0 \\ R_0 + (e^{i\theta})(x - R_0) & \text{if } x > R_0. \end{cases} \tag{21}$$

This method is extremely easy to use since it only requires multiplying the derivative matrix by the complex scalar $e^{-i\theta}$. More recently, some authors [10–12] have recommended using a differentiable contour instead, as the point of non-analyticity in the above contour has been reported to lead to stability and convergence problems. On choosing a smooth contour such as a hyperbola, the Schrödinger operator can become much more complicated. In our experience, numerical problems arising from the method of complex exterior scaling are a consequence of using a centered difference discretization across the point of non-analyticity, R_0. This trouble does not appear if spectral elements are used, provided that the point R_0 occurs at the boundary between elements. If this is the case, spectral convergence is recovered.

4.3. Scattering states and tunneling

Scattering states belong to the continuous spectrum and for a one-dimensional problem, they can be thought of as right- or left-propagating waves. Unlike resonances, scattering states are physical solutions, but are not true eigenfunctions since they do not satisfy two-point boundary conditions. Traditionally, the scattering states and tunneling probability have been computed using shooting by approximating the potential as piecewise constant [6] or linear [7]. Here we use the same approach, except that the spectral method is optimal because instead of approximating the potential as piecewise constant or linear, any piecewise smooth function is allowed.

Here we describe how to compute the right-propagating scattering wavefunction for a single element. Generalization to multiple elements is similar to the case for the eigenvalue problem discussed previously and this can be solved rapidly since it is a block-tridiagonal system. Both the solution and its derivative are prescribed as boundary values at the right endpoint of the domain. This radiation condition arises from the asymptotic plane-wave behavior of the solution which leads to an initial value problem. Using the scaled functions and parameters as before,

$$u(+1) = 1, \quad u'(+1) = ik_r, \quad k_{r,l} = \sqrt{\lambda - q_{r,l}}. \tag{22}$$

To compute the Legendre expansion coefficients for the solution, one must solve the integration-preconditioned system

$$\begin{pmatrix} \boldsymbol{\delta}_+ \\ \boldsymbol{\nu}_+ \\ -\mathbf{I}_{[2]} + \mathbf{B}_{[2]}^2[\mathbf{Q} - \lambda\mathbf{I}] \end{pmatrix} \hat{\mathbf{u}} = \begin{pmatrix} 1 \\ ik_r \\ \mathbf{0} \end{pmatrix} \tag{23}$$

The approach is similar for left-propagating solutions, except that initial values are imposed at the left endpoint and ik_r is replaced by $-ik_l$. Once the solution vector, $\hat{\mathbf{u}}$ [2] is computed, the reflection and tunneling probabilities are calculated from

$$R(\lambda) = \left| \frac{(ik_l \boldsymbol{\delta}_- - \boldsymbol{\nu}_-)\hat{\mathbf{u}}}{(ik_l \boldsymbol{\delta}_- + \boldsymbol{\nu}_-)\hat{\mathbf{u}}} \right|^2, \quad T(\lambda) = 1 - R(\lambda). \tag{24}$$

5. Numerical inner products

Frequently in quantum mechanics, one is interested in computing inner products such as a transition probability or the expectation value of an operator. Here we show that when the spectral tau method is used to compute the expansion coefficients for the eigenfunctions of the Hamiltonian, inner products can be computed rapidly with quadrature accuracy without requiring a transformation to point space. Now suppose one wishes to compute the inner product

$$\langle u \mid v \rangle = \int_{-1}^{+1} u^*(x) v(x)\, \mathrm{d}x. \tag{25}$$

The numerical integration is carried out using

$$\langle u \mid v \rangle = \hat{\mathbf{u}}^* \mathbf{M} \hat{\mathbf{v}} \tag{26}$$

where $\mathbf{M}$ is just the Legendre mass matrix, which is diagonal, with entries $m_{jj} = \frac{2}{2j+1}$. In modeling optoelectronic devices, photoabsorption and emission are computed by finding the matrix elements of the momentum operator. Using the Legendre tau discretization, this computation is extremely fast and accurate and can be performed for many transitions simultaneously. For the momentum operator, the momentum matrix is simply

$$\langle u_f \mid \hat{p} \mid u_i \rangle = i\hbar \hat{\mathbf{U}}^* \mathbf{M} \mathbf{D} \hat{\mathbf{U}}. \tag{27}$$

Here $\hat{\mathbf{U}}$ is a set of computed eigenvectors. For a multi-element scheme, the inner products are computed element by element. Remarkably, no additional error is introduced in numerically computing the momentum matrix elements, as the Legendre–Gauss–Lobatto quadrature is exact for polynomials of order $2N - 1$.

6. Concluding remarks

We have presented a fast and efficient method for solving the TISE for an arbitrary semiconductor heterostructure. By expanding in terms of orthogonal polynomials, we obtain a matrix representation of the Hamiltonian from which we may simultaneously compute as many eigenfunctions and eigenvalues as desired. This offers a substantial advantage over more prevalent shooting methods as we do not need to hunt for eigenvalues because that work is performed by a matrix eigensolver routine. For all examples, the MATLAB® function `eig` was used to obtain eigenvalues and eigenvectors. We have also shown that the spectral method requires much smaller matrices than the finite difference method to achieve comparable error. Frequently, the spectral matrix size is orders of magnitude smaller. Integration preconditioning was introduced into the Schrödinger eigenproblem, giving a sparse quasi-banded structure to the matrices.

The spectral element method was then extended to incorporate unbounded domains through rational mapping. The mapping demonstrated superior convergence over the more traditional domain truncation approach. We discussed the phenomena of resonances and the difficulties of computing them. Using a complex coordinate scaling for the end elements, we showed that one may solve the TISE on a new contour that need not be differentiable. Additionally, the scattering states and tunneling probability were shown to be easily obtainable by formulating a spectral element initial value problem. Finally, we demonstrated that one may easily compute inner products and expectations of operators in the spectral domain using simple matrix vector multiplication.

Acknowledgements

This work was supported by DOE Basic Energy Sciences Grant DE-FG03-02ER46014 and DOE SNL Grant 66513.

References

[1] F.L. Serzhenko, N.F. Johnson, Resonant phenomena involving bound-to-continuum transitions in quantum wells, Applied Physics Letters 63 (25) (1993) 3467–3469.
[2] A.Z. Capri, Nonrelativistic Quantum Mechanics, World Scientific, Singapore, 2002.
[3] K.R. Lefebvre, A.F.M. Anwar, Redistribution of the quantum well density of states under the influence of an electric field, Semiconductor Science and Technology 12 (1997) 1226–1230.
[4] T. Shibata, Absorbing boundary conditions for the finite-difference time-domain calculation of the one-dimensional Schrödinger equation, Physical Review B 43 (8) (1991) 6760–6763.
[5] I. Alonso-Mallo, N. Reguera, Weak ill-posedness of spatial discretizations of absorbing boundary conditions for Schrödinger-type equations, SIAM Journal of Numerical Analysis 40 (1) (2002) 134–158.
[6] A. Peres, Transfer matrices for one-dimensional potentials, Journal of Mathematical Physics 24 (1983) 1110–1119.
[7] M. Čížek, J. Horáček, On shooting methods for calculation of potential resonances, Journal of Physics A 29 (1996) 6325–6342.
[8] M.L. Zambrano, J.C. Arce, Stark-resonance densities of states, eigenfunctions, and lifetimes for electrons in GaAs/(Al,Ga)As quantum wells under strong electric fields: An optical-potential wave-packet propagation method, Physical Review B 66 (2002) 155340 1–9.
[9] B. Simon, The definition of molecular resonance curves by the method of complex exterior scaling, Physics Letters 71A (2) (1979) 211–214.
[10] M.V. Ivanov, Complex rotation in two-dimensional mesh calculations for quantum systems in uniform electric fields, Journal of Physics B: Atomic, Molecular and Optical Physics 34 (2001) 2447–2473.
[11] M.F. Levy, Perfectly matched layer truncation for parabolic wave equation models, Proceedings of the Royal Society of London A 457 (2001) 2609–2624.
[12] T. Hagstrom, New results on absorbing layers and radiation boundary conditions, in: M. Ainsworth, P. Davies, D. Duncan, P. Martin, B. Rynne (Eds.), Topics in Computational Wave Propagation, Springer-Verlag, 2003, pp. 1–42.
[13] H.V. McIntosh, Quantization as an eigenvalue problem, in: E.M. Loebl (Ed.), Group Theory and its Applications, Academic Press, New York, 1975.
[14] C. Canuto, M.Y. Hussaini, A. Quarteroni, T.A. Zang, Spectral Methods in Fluid Dynamics, Springer-Verlag, New York, 1987.
[15] P. Midy, O. Atabek, G. Oliver, Complex eigenenergy spectrum of the Schrödinger equation using Lanczos' tau method, Journal of Physics B: Atomic, Molecular, and Optical Physics 26 (1993) 835–853.
[16] M. Braun, S.A. Sofianos, D.G. Papageorgiou, I.E. Lagaris, An efficient Chebyshev–Lanczos method of obtaining eigensolutions of the Schrödinger equation on a grid, Journal of Computational Physics 126 (1996) 315–327.
[17] C. Lanczos, Applied Analysis, Prentice-Hall, Englewood Cliffs, NJ, 1956.
[18] G.H. Golub, C.F. van Loan, Matrix Computations, Johns Hopkins University Press, 1996.
[19] D. Gottlieb, S. Orszag, Numerical Analysis of Spectral Methods, SIAM, Philadelphia, PA, 1977.
[20] E.A. Coutsias, T. Hagstrom, D. Torres, An efficient spectral method for ordinary differential equations with rational function coefficients, Mathematics of Computation 65 (214) (1996) 611–635.
[21] E.A. Coutsias, T. Hagstrom, J.S. Hesthaven, D. Torres, Integration preconditioners for differential operators in spectral τ-methods, in: Proceedings of the International Conference on Spectral and High Order Methods, ICOSAHOM'95, Houston, USA, 1995, pp. 21–38.
[22] R.B. Lehoucq, D.C. Sorensen, C. Yang, ARPACK Users' Guide: Solution of Large-scale Eigenvalue Problems with Implicitly Restarted Arnoldi Methods, in: Software, Environments, and Tools, Society for Industrial and Applied Mathematics (SIAM), Philadelphia, PA, 1998.
[23] G. Szegö, Orthogonal Polynomials, vol. 23, American Mathematical Society Colloquium Publications, 2003.
[24] D. Gottlieb, C.W. Shu, On the Gibbs phenomenon and its resolution, SIAM Review 39 (1997) 644–668.
[25] B. Guo, J. Shen, Z. Wang, Chebyshev rational spectral and pseudospectral methods on a semi-infinite interval, International Journal for Numerical Methods in Engineering 53 (2002) 65–84.
[26] W.P. Rheinhardt, Complex coordinates in the theory of atomic and molecular structure and dynamics, Annual Review of Physical Chemistry 33 (1982) 223–255.